Experimental Determination of Critical Threshold in Electron Transport on Tore Supra

G. T. Hoang, C. Bourdelle, X. Garbet, G. Giruzzi, T. Aniel, and M. Ottaviani
Département de Recherches sur la Fusion Contrôlée, Association Euratom-CEA, CEA Cadarache, 13108 Saint-Paul-lez-Durance, France

W. Horton and P. Zhu
Institute for Fusion Studies, The University of Texas at Austin, Austin, Texas 78712

R. V. Budny
Princeton Plasma Physics Laboratory, Princeton University, Princeton, New Jersey 08543
(Received 17 November 2000; published 4 September 2001)

In Tore Supra plasmas with fast wave electron heating, a critical threshold in the electron temperature gradient (∇T_e) is clearly observed, i.e., a finite value of ∇T_e for which the turbulent heat diffusivity vanishes. The radial profile of this critical gradient is experimentally determined from a set of discharges characterized by similar plasma parameters with fast wave powers ranging from 0.75 to 7.4 MW. The dependence of the electron heat flux on the gradient length is found to be offset linearly. The offset term increases linearly with the ratio of the local magnetic shear to the safety factor.

DOI: 10.1103/PhysRevLett.87.125001 PACS numbers: 52.55.Fa, 52.25.Fi, 52.65.Tt

Temperature gradients are a universal agent for driving both laminar and turbulent convection in fluids, gases, and plasmas. In weakly collisional plasmas with auxiliary heating sources it is natural to expect two types of temperature gradient driven convections: (i) in high power neutral beam injection heating, where the ion temperature gradient (ITG) mode can likely explain many features of the turbulent plasma with correlation lengths ranging from 3 to 30 ion gyroradii; (ii) in high power electron heating driving up electron temperature gradients (∇T_e). In this case, there are two main candidates to explain the electron transport; trapped electron modes (TEM), characterized by wave numbers in the same range as ITG, and the smaller-scale electron temperature gradient (ETG) modes. For both ITG and ETG, many anomalous transport models based on either stability theory or numerical simulations [1–10] predict a critical threshold, above which the turbulence develops and the heat transport increases.

In previous electron heating experiments, the existence of such a threshold is suggested by the electron transport analysis [11,12] and by the measurements of both density and magnetic fluctuations [13,14]. However, these experiments did not provide the radial profile of the critical gradient and its dependence on the plasma parameters. These are necessary for the electron transport modeling, a relevant issue for reactor-grade plasmas dominated by electron heating due to collisional relaxation of α particles. In general, the profile and parametric dependence of the electron threshold given by either theoretical expressions [10] or formulas based on dimensional analysis, corroborated by fits of given plasma discharges [5], are used for transport simulations.

Among the various plasma parameters, electron transport is known to be particularly sensitive to the magnetic configuration, i.e., to the safety factor (q) and to the magnetic shear (s). In order to isolate this crucial dependence, experiments are needed in which rotation effects induced by ion heating or direct momentum injection are negligible. Moreover, sawteeth should be absent or weak, and the electron heat source should be spatially well localized and intense enough to allow exploration of a significant range of ∇T_e. All these conditions are met in fast wave electron heating (FWEH) experiments on Tore Supra [15]. The electron transport analysis of these FWEH discharges allows, for the first time, an accurate experimental determination of the radial profile of the electron critical threshold, and of its dependence on s and q.

To accomplish this program, a data set of ^{4}He plasmas heated by FW has been used, carefully chosen in order to keep most plasma parameters constant during an extensive wave power scan. The FWEH scenario was obtained by minimizing the parasitic damping of the ions in order to maximize the absorption of the wave by the electrons [15]. The FW power (P_{FW}) is directly absorbed by thermal electrons, and no fast particles were present in these discharges. The FW power deposition profile, computed with the codes ALCYON [16] and PION [17], is localized inside $r/a = 0.2$ and more than 90% of P_{FW} is absorbed by the electrons. These hot electron plasmas [$T_e(0) = 1.9$–5.2 keV, Fig. 1(a)] are characterized by weak electron-ion collisional coupling. The combination of core localized power deposition and weak coupling to the ions gives an unusually clear electron transport channel for 50 to 100 electron energy confinement times. A series of shots with the same density (n_e) and q profiles (Fig. 1b) was performed at plasma current $I_p = 0.65$ MA and toroidal field $B = 2.2$ T. For each radial position, the variations ($<10\%$) of n_e and q are smaller than their absolute error bars. The range of the total power is 1.5–7.5 MW (Ohmic power $P_{\mathrm{OH}} = 0.1$–0.75 MW and $P_{\mathrm{FW}} = 0.75$–7.4 MW);

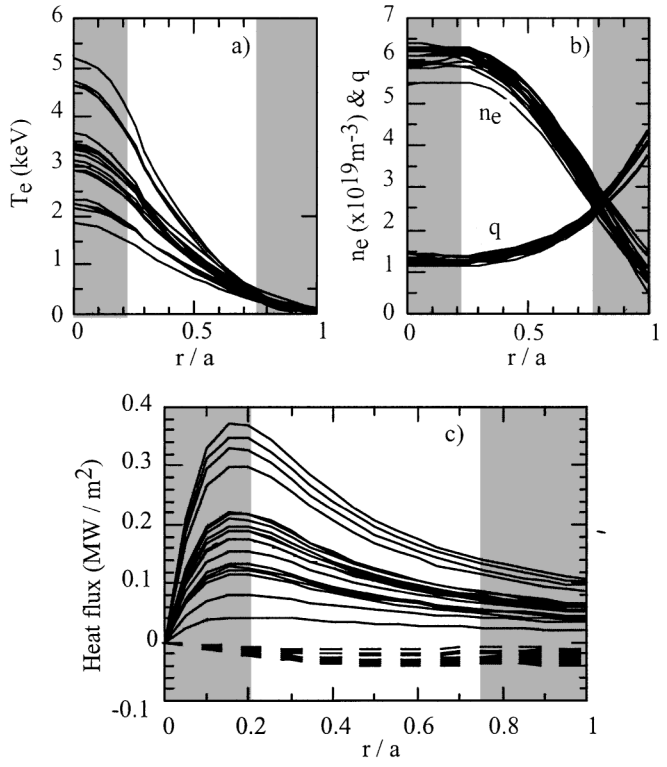

FIG. 1. Radial profiles of (a) electron temperature; (b) electron density and safety factor; (c) heat flux (full: FW coupled to electrons + Ohmic; dashed: radiation and electron-ion losses).

21 time slices in the stationary phases of 8 discharges were selected. The large variation of P_{FW} allows an accurate scan of the electron temperature gradient from 1 to 12 keV/m. We limit our analysis to normalized radii (r/a) between 0.2 and 0.75, since the plasma center is dominated by the heating source, and the power balance at the edge is affected by uncertainties from radiation and recycling. The q profiles are measured by the polarimetry, with an error in the range of 10% (at midradius) and 25% (at the center). The relative error of T_e (28 radial points measured by Thomson scattering and electron cyclotron emission diagnostics) is less than 20%. $T_i(0)$, ranging from 1.3 to 1.8 keV within the error bars of 20%, is measured by the Doppler shift of the Fe^{24+} line.

Power balance analysis shows an offset linear dependence of the electron heat flux (q_e) on ∇T_e as shown in Fig. 2a. This indicates the existence of a critical electron temperature gradient (∇T_c), for which the turbulent heat diffusivity vanishes. In Fig. 2a, q_e is varied by a factor of about 10: 0.03/0.3 MW m^{-2} $(r/a = 0.2)$ and 0.007/0.08 MW m^{-2} $(r/a = 0.75)$. The profile of T_i, computed by transport code, is constrained by the measured total thermal energy content and $T_i(0)$. The uncertainty on q_e, mainly related to the electron-ion equipartition term, is less than 20%, except for $r/a \geq 0.5$ at low P_{FW} (Fig. 1c). The radiation losses do not significantly contribute to the uncertainties on q_e, since most of the radiated power (15%

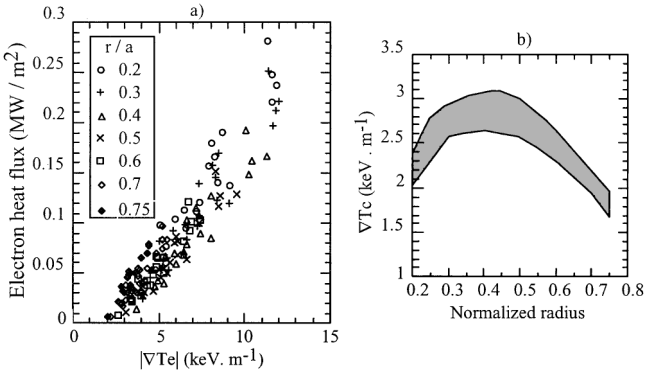

FIG. 2. (a) Electron heat flux versus ∇T_e at various radii. (b) Radial profile of critical gradient, deduced from linear extrapolation.

to 20% of the total power) comes from $r/a > 0.75$ (up to 80%). For each radial position, ∇T_c is determined by a linear fit of q_e. Despite its large error bar (up to 100%) the lowest heat flux point in Fig. 2a does not influence this linear fit at all. Best fits, with slopes almost independent of r (0.50 ± 0.15), give ∇T_c between 2–3 keV/m; its profile is shown in Fig. 2b. Of course, the dependence of q_e on $|\nabla T_e|$ could be reproduced by a power fit. However, in this case, the modeling of electron transport becomes more complicated, since the exponent itself would have a strong radial variation, from 1.5 $(r/a = 0.2)$ to 2.6 $(r/a = 0.75)$.

A similar dependence also appears versus the gradient length ($L_{T_e} = |T_e/\nabla T_e|$), as shown in Fig. 3a. At a given radius, L_{T_e} has a weak variation (within the error bar), while q_e is increased by a factor of 10. The variation of L_{T_e} is around 30%, except for $a \geq 0.7$ (60%) where the error bars are large. This trend is similar to the observation of the so-called "stiff" T_e profile in ASDEX experiments [12], in which L_{T_e} is almost constant when q_e varies by a factor ≤ 3.

The main finding of this work is that the Tore Supra FW transport database is optimally represented by an offset linear formula, independent of the density (Figs. 4a and 4b),

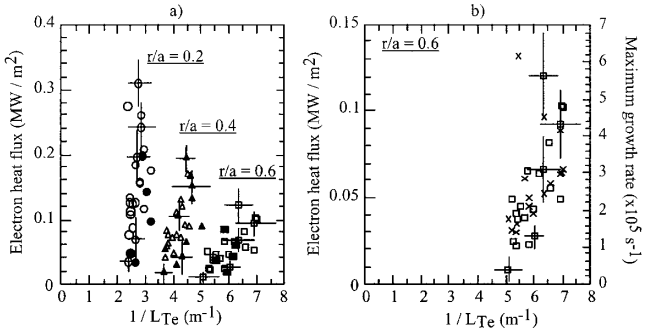

FIG. 3. (a) Electron heat flux versus $1/L_{T_e}$ at various radii. Full symbols correspond to another series of discharges performed at different values of n_e and q [$n_e(0) = 4 \times 10^{19}$ m^{-3}, $q_{\mathrm{edge}} = 6.5$]. (b) Maximum linear growth rates (crosses) and electron heat flux (squares) versus $1/L_{T_e}$.

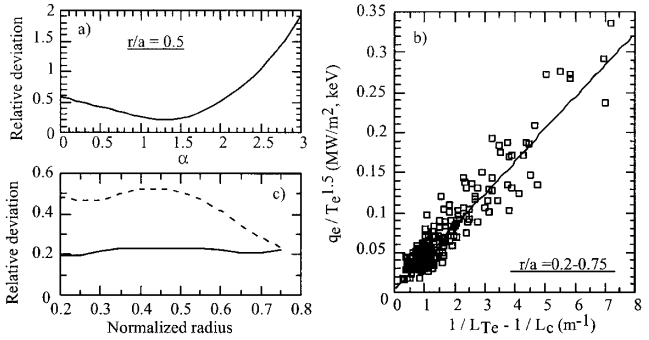

FIG. 4. Normalized heat flux q_e/T_e^{α} as a function of $(1/L_{T_e} - 1/L_c)$: (a) Relative deviation of the linear fit as a function of α; (b) Linear fit with $\alpha = 1.5$; (c) Relative deviation of the linear fit with $\alpha = 1.5$ (solid), compared with the case $q_e/(n_e \cdot T_e^{1.5})$ (dashed).

$$q_e \propto T_e^{\alpha}\left(\frac{1}{L_{T_e}} - \frac{1}{L_c}\right), \tag{1}$$

where $1/L_c$ is determined, for each radius, by a linear extrapolation of q_e versus $1/L_{T_e}$ (Fig. 3a). As shown in Fig. 4a, the best fit corresponds to $\alpha \approx 1.5$. The dependence on T_e is compatible with the Gyro-Bohm model, based on the electromagnetic ETG turbulence [10]:

$$q_e^{\mathrm{em}} = C_{\mathrm{em}} q^{\nu} n_e \left(\frac{c}{\omega_{\mathrm{pe}} R}\right)^2 \left(\frac{R}{L_{T_e}}\right)^{3/2} v_{\mathrm{th},e} T_e \left(\frac{R}{L_{T_e}} - \frac{R}{L_c}\right). \tag{2}$$

The linear fit of the normalized heat flux, $q_e^* = q_e/T_e^{1.5}$, gives a relative deviation of about 20% for all radii (Fig. 4c, solid line). Conversely, the relative deviations reach up to 50% when q_e is normalized to $n_e T_e^{2.5}$, according to Gyro-Bohm electrostatic models (Fig. 4c, dashed line).

Stability analysis of these discharges has been done with a linear electrostatic gyrokinetic code [18]. Passing and trapped ions and electrons are taken into account, which means that ITG, TEM, and ETG modes are included. The microinstabilities are found to be dominated by TEMs ($k_\theta \delta_e \approx 0.5$, δ_e being the banana width). The growth rate spectra at given radii are computed with the experimental temperature, density, and q profiles. The maximum growth rates ($\gamma^{\max}$) are calculated over each spectrum at a given radial position. The dependence of $\gamma^{\max}$ upon L_{T_e} is very similar to the trend observed in q_e (Fig. 3b).

In order to verify that the introduction of an offset term in the empirical conductivity seems unavoidable, the following alternative expression, with no offset but a more general power-law dependence, has been considered:

$$q_e \propto T_e^{\alpha}\left(\frac{1}{L_{T_e}}\right)^{\beta} \tag{3}$$

with or without the density dependence. In this case we found that a value of β around 3, and $\alpha \approx 1.5$, with no density dependence, could fit the data near the center (Fig. 5). However, the fit is not as good as Eq. (1), when

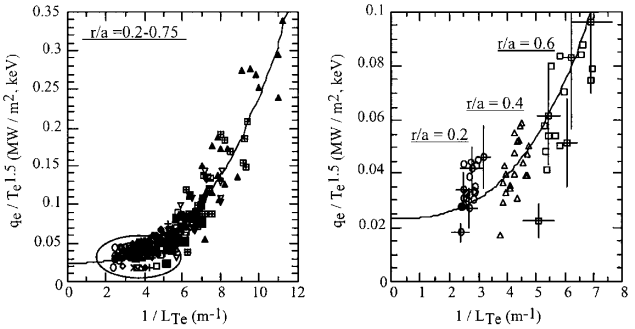

FIG. 5. Normalized heat flux $q_e/T_e^{1.5}$ as a function of $1/L_{T_e}$ for various radii. Solid line corresponds to the fit $(1/L_{T_e})^{(2.8\pm0.2)}$.

carried out at all the radial locations, since one would need to vary β as a function of radius in the range from 1.6 to 3.2. The same problem appears when normalizing to the density $q_e^* = q_e/n_e T_e^{2.5}$ (as suggested by the electrostatic ETG model).

Next, the parametric dependence of the threshold length L_c has been studied. No significant dependences on n_e, q, and density gradient are observed. Indeed, as shown in Fig. 3, the offset value at a given radius, corresponding to two series of discharges characterized by completely different n_e and q profiles, but the same ratio s/q, is practically unchanged. This suggests that the radial variation of $1/L_c$, displayed in Fig. 3, is mainly related to the ratio s/q. Its radial profile is shown in Fig. 6a. The dimensionless parameter R/L_c, deduced from both power balance and stability analyses, is plotted versus s/q in Fig. 6b ($R = 2.28$ m, being the major radius), showing that $1/L_c$ increases linearly with s/q. Critical values deduced from the calculation of the linear electrostatic growth rates are somewhat lower than the values obtained from the power balance analysis. A possible explanation is that the experimental threshold is determined by nonlinear effects, and therefore higher than the linear value, as found in ITG simulations [9]. A best fit of the data of the power balance analysis gives an offset linear formula

$$\frac{R}{L_c} = 5(\pm 1) + 10(\pm 2)\,\frac{|s|}{q}\,. \tag{4}$$

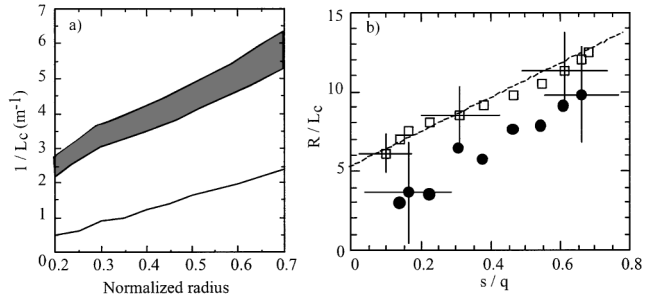

FIG. 6. (a) Radial profile of $1/L_c$, deduced from power balance analysis, compared with the ETG formula given by Eq. (5) (solid line). (b) R/L_c versus s/q (squares: power balance; circles: stability analysis; dashed line: fit).

This is consistent with an improved confinement due to increasing s in the pressure gradient region (high plasma inductance l_i mode in TFTR [19], DIII-D [20], JET [21], and Tore Supra [11,22]). A similar dependence on s/q is predicted by the model used in Ref. [10], according to the Hahm and Tang formula [6]:

$$\frac{R}{L_c^{\mathrm{ETG}}} = 1.88\,\frac{|s|}{q}\left(1 + Z_{\mathrm{eff}}\,\frac{T_e}{T_i}\right). \tag{5}$$

Despite the absence of the offset term (probably due to toroidal effects which are not taken into account in the model), this formula reproduces the radial profile of the experimental threshold well (Fig. 6a). However, it gives a value almost twice lower than the experimental one. This could be explained by the fact that the constant (1.88) in Eq. (5) was obtained following the ITG mode analysis given in [6], adapted to the ETG mode. Recently, the results of nonlinear gyrokinetic simulations of toroidal turbulence driven by the ITG [9] also indicated this dependence, with an ion critical threshold ($R/L_{T_i} = 5$–6) close to our experimental value.

In summary, a critical electron temperature gradient is clearly shown to exist in Tore Supra hot electron plasmas, with a weak radial dependence ($\nabla T_c = 2$–$3\ \mathrm{keV\,m^{-1}}$). The results also support the critical gradient length models [Eq. (1)]. No significant dependence of q_e on the density is found, consistent with the electromagnetic ETG turbulence model. We stress that other popular turbulence models do not give a comparable agreement. For example, the collisionless ITG + TEM branch has the wrong density dependence and similarly for the electrostatic ETG. The dissipative version of TEMs would have the right density dependence but also a too strong temperature dependence, and above all, the theory is not valid in the collisionality regime of the FW discharges.

Above the critical threshold $1/L_c$, the electron heat transport strongly increases: the variation of gradient length is very weak ($\approx$30%) by varying the heat flux by a factor of 10. This could explain why many strong power dependence models, without the offset term, can simulate electron transport with acceptable discrepancies when the temperature gradient exceeds the critical value. The parameter $1/L_c$ is found to have an offset-linear dependence on the ratio s/q [Eq. (4)], suggesting the essential role of magnetic shear in electron transport. This magnetic shear dependence is consistent with the observation of improved confinement with increasing magnetic shear in the confinement zone (high-l_i regime) in many tokamaks. The decrease of the heat diffusivity could be ascribed to the reduction of L_c for increasing shear.

The diligent support of the Tore Supra team is gratefully acknowledged.

[1] C. S. Liu, M. N. Rosenbluth, and C. W. Horton, Phys. Rev. Lett. **29**, 1489 (1972).
[2] F. L. Hinton *et al.,* in *Plasma Physics and Controlled Nuclear Fusion Research, Proceedings of the 8th International Conference, 1980* (IAEA, Vienna, 1981), p. 365.
[3] W. Horton *et al.,* Phys. Fluids **31**, 2971 (1988).
[4] F. Romanelli, Phys. Fluids B **1**, 1018 (1989).
[5] P. H. Rebut *et al.,* in *Plasma Physics and Controlled Nuclear Fusion Research, Proceedings of the 12th International Conference, 1988* (IAEA, Vienna, 1989), p. 191.
[6] T. S. Hahm and W. M. Tang, Phys. Fluids B **1**, 1185 (1989).
[7] W. Dorland *et al.,* in *Plasma Physics and Controlled Nuclear Fusion Research, Proceedings of the 15th International Conference, 1994* (IAEA, Vienna, 1995), p. 463.
[8] B. W. Stallard *et al.,* Phys. Plasmas **6**, 1978 (1999).
[9] A. M. Dimits *et al.,* in Proceedings of the 18th IAEA Fusion Energy Conference, 2000 (to be published) [IAEA-CN-77/THP1/03, 2000].
[10] W. Horton *et al.,* Phys. Plasmas **7**, 1494 (2000).
[11] G. T. Hoang *et al.,* Nucl. Fusion **38**, 117 (1998).
[12] F. Ryter *et al.,* in Proceedings of the 18th IAEA Fusion Energy Conference, 2000 (to be published) [IAEA-CN-77/EX2/2, 2000].
[13] P. Devynck *et al.,* Plasma Phys. Controlled Fusion **39**, 1355 (1997).
[14] L. Colas *et al.,* Nucl. Fusion **38**, 903 (1998).
[15] B. Saoutic *et al.,* Plasma Phys. Controlled Fusion **36**, Suppl. B, 123 (1994).
[16] A. Bécoulet *et al.,* Phys. Plasmas **1**, 2908 (1994).
[17] L.-G. Eriksson *et al.,* Nucl. Fusion **33**, 1037 (1993).
[18] C. Bourdelle *et al.,* in Proceedings of the 27th European Conference, Budapest, 2000 (to be published).
[19] M. C. Zarnstorff *et al.,* in *Plasma Physics and Controlled Nuclear Fusion Research, Proceedings of the 13th International Conference, 1990* (IAEA, Vienna, 1991), p. 109.
[20] J. R. Ferron *et al.,* in *Proceedings of the Joint ICCP-19th European Conference on Controlled Fusion and Plasma Physics, Innsbruck, 1992* (European Physical Society, Petit-Lancy, 1992), Vol. 16C, Pt. 1, p. 55.
[21] C. D. Challis *et al.,* Nucl. Fusion **32**, 2217 (1992).
[22] G. T. Hoang *et al.,* Nucl. Fusion **34**, 75 (1994).